Inorganic Chemistry

ARTICLE

pubs.acs.org/IC

Porous CdTe Nanocrystal Assemblies: Ligation Effects on the Gelation Process and the Properties of Resultant Aerogels

Qinghong Yao and Stephanie L. Brock*

Department of Chemistry, Wayne State University, Detroit, Michigan 48202, United States

Supporting Information

ABSTRACT: Highly porous CdTe nanoarchitectures (aerogels) were prepared by sol−gel assembly of discrete nanocrystals followed by supercritical CO_2 drying. CdTe nanocrystal surface functionalization (either phosphine oxide or thiolate) is found to be immaterial to oxidation induced gel formation suggesting that the standard thiolate capping procedure is not a necessary step in the gelation process. On the basis of this observation, and reduction induced dispersion of the gel network, the exposure of reactive sites and the subsequent surface oxidation reaction to form polychalcogenide linkages are key steps in the gelation mechanism. Consequently, CdTe aerogels exhibit similar physicochemical properties, regardless of original ligating functionality. The aerogels are mesoporous, with surface area >100 m^2/g, and exhibit an optical bandgap of 1.92 eV, consistent with quantum confinement within the 3-D linked network. Photoluminescence is suppressed in the aerogels, but can be partially recovered upon heating.

INTRODUCTION

CdTe nanocrystals (NCs) have received considerable attention due to their size-dependent emission properties, spanning from the UV through the near IR, as well as their large window for absorbance (λ < 825 nm, based on a bulk band gap of 1.5 eV) and high extinction coefficient (>1 × 10^5 cm^{-1} M^{-1}).[1] These factors, combined with the documented synthetic methods for obtaining high-quality CdTe NCs with control of size,[1−3] shape,[3,4] and surface chemistry[5,6] have made them promising materials for many applications, such as light emitting diodes (LEDs),[7−9] photovoltaic devices,[10,11] and sensors.[12,13] However, applications that rely on electrically connected systems require the discrete nanocrystals accessible by solution phase strategies to be assembled into "wired" superstructures while retaining the inherent properties of primary nanocrystals. Furthermore, for certain applications (e.g., sensing and photocatalysis), the assembled nanostructures should be open and accessible to small molecules to facilitate reactions occurring on the surface of nanocrystals.

Metal chalcogenide (MQ) aerogels (AGs) are composed of physically connected nanoscale building blocks without organic spacers and represent one class of semiconducting inorganic porous nanostructure.[14] The synthesis of MQ aerogels developed by Brock and co-workers is based on a two-step sol−gel synthesis route and is generally applicable to the assembly of a range of MQ compositions, including CdS, PbS, ZnS, CdSe, and CdSe/ZnS,[15−17] in addition to heterocomposites between noble metal nanoparticles and CdS NCs.[18,19] A typical synthetic route involves the following: synthesis of primary phosphine oxide capped NCs, surface ligand exchange with thiolates, gelation of the thiolate-capped NCs by partial removal of thiolate capping groups from the nanocrystal surface to form a wet gel, and supercritical drying of the wet gel to yield an aerogel. The removal of surface thiolate groups can be achieved by the chemical oxidation method by addition of oxidants [e.g., H_2O_2 or tetranitromethane (TNM)] or photo-oxidation ($h\nu/O_2$). The aerogels that result from supercritical drying retain 90−95% of the wet gel volume and exhibit large surface areas and high porosities, similar to the characteristics of base-catalyzed silica aerogels. They are macroscopic assemblies in the form of bulk monoliths and retain the inherent properties of the primary nanobuilding blocks, specifically, the quantum confined optical-electric properties.[20]

The gelation mechanism for the assembly of thiolate (11-mercaptoundecanoic acid) capped metal chalcogenide NCs (CdSe, CdS, and ZnS) has been recently reported by Brock and co-workers.[21] Briefly, the study revealed that, during gelation, the thiolate ligands were either chemically oxidized or photo-oxidized to produce soluble disulfide species, thereby exposing the nanocrystal surface. The decomplexed Cd^{2+} ions were then dispersed in solution via solvation, leaving a chalcogenide rich particle surface. By further oxidation, the Q^{2-} (Q = S, Se) ions were oxidized into $Q^{\cdot -}$ fragments, which can link the particles together to form a gel network supported by $(Q_2)^{2-}$ or $(Q_n)^{2-}$ fragments. The polychalcogenide bonding in the aerogels was confirmed by Raman and X-ray photoelectron spectroscopies.[21] Consistent with the redox mediated gelation, the resultant gels can be redispersed by addition of reducing agents (e.g., thiols, $NaBH_4$). This oxidative gelation approach is also expected to be applicable to the assembly of CdTe NCs, because tellurides are more easily oxidized than sulfides or selenides.

Received: June 21, 2011
Published: September 28, 2011

ACS Publications © 2011 American Chemical Society

A few studies have been performed on the assembly of CdTe NCs. Kotov and co-workers reported self-assembly of thiolate stabilized CdTe NCs into 1D nanowires[22] or 2D sheets[23] via partial depletion of thiolate stabilizers by washing with methanol. In contrast to the oxidization induced gelation process employed by the Brock group, the assembly was reported to occur in the absence of an external oxidant and in the dark, precluding photo-oxidation induced processes (recently, it has been shown that photo-oxidation can be used to make helical ribbons from the straight ribbons formed in the dark[24]). Gaponik and Eychmüller demonstrated 3D assembly of thioglycolic acid (TGA)-capped CdTe NCs into gels and AGs.[25] They used aging, chemical oxidation, and photochemical methods to induce gelation and produced the aerogel by supercritical drying. The CdTe gels and aerogels were found to exhibit the classic pearl-necklace architecture and were highly luminescent. However, other physical properties (e.g., surface area, crystal phase, and elemental composition) were not evaluated. More recently, Eychmüller and co-workers reported 3D assembled nanostructures containing "piled-up" CdTe@Cd-TGA complex nanowires.[26] Without employing an oxidative process, the assembly was achieved by partial removal of TGA capping groups in the presence of ethanol and a highly concentrated salt. The CdTe NCs are essentially embedded in the Cd-TGA gel matrix and are highly luminescent. Metal cross-linking of tetrazolyl analogues leads to similar assemblies.[27]

The present paper provides a detailed study of CdTe gel formation by chemical oxidation as a function of surface ligation and the consequences for the nature of the resultant aerogels. We demonstrate that the common thiolate-capping approach is not a prerequisite to gel formation, and reveal, for the first time, the physicochemical properties of CdTe aerogels in terms of structure, morphology, surface area, and porosity, as well as optical properties.

EXPERIMENTAL SECTION

Materials. Trioctylphosphine oxide (TOPO, 90%), cadmium oxide (99.99%), tellurium powder (99.9%), trioctylphosphine (TOP, 90%), 11-mercaptoundecanoic acid (MUA, 95%), 16-mercaptohexadecanoic acid (MHA, 90%), and tetranitromethane (TNM) were purchased from Sigma-Aldrich. Tetramethylammonium hydroxide pentahydrate (TMAH, 99%) was purchased from Acros. *N*-Tetradecylphosphonic acid (TDPA, 98%) was purchased from Alfa-Aesar. Ethyl acetate, toluene, acetone, and methanol were purchased from Fisher Scientific.

Synthesis of Cadmium Telluride Aerogels. *Synthesis of TOPO-Capped CdTe Nanocrystals.* TOPO-capped CdTe NCs were prepared by Peng et al.'s method[28] with slight modification. A typical synthesis procedure occurs as follows. A mixture of CdO powder (0.0514 g), TDPA (0.1116 g), and TOPO (3.7768 g) was loaded in a 250 mL Schlenk flask and slowly heated to 320 °C under argon flow to obtain a clear solution. The temperature of the reaction solution was reduced to 270 °C, and a tellurium precursor (0.0664 g of tellurium powder dissolved in 2.4 mL of TOP) was quickly injected. The reaction solution was cooled down to 100 °C immediately after the injection and slowly heated back to 240 °C (10 °C per 10 min) where it was left for 1 h and then allowed to cool to room temperature. The resultant CdTe NCs were dispersed in toluene and precipitated with methanol. After centrifugation, the precipitate of CdTe NCs was redispersed in toluene, and the resultant CdTe sol was centrifuged one more time to remove the insoluble byproducts and impurities. The subsequent CdTe sol was precipitated with methanol to obtain the purified TOPO-capped CdTe NCs, which were subjected to direct gelation or the thiolate ligand exchange procedure. For direct gelation of TOPO-capped CdTe NCs, the purified nanocrystals were redispersed in toluene and reprecipitated by methanol twice more before final dispersion in 16 mL of toluene.

MHA-Capping of CdTe Nanocrystals. MHA-capped CdTe NCs were prepared following a modification of the method reported by Aldana et al.[29] Briefly, 0.5770 g of MHA was dissolved in 10 mL of methanol, and the pH was adjusted to >10 using TMAH. In the absence of light, the resulting solution was added to TOPO-capped CdTe NCs prepared from one batch of the reaction described in the proceeding section and shaken vigorously to ensure that the CdTe NCs were dispersed completely. The resultant MHA-capped CdTe NCs were precipitated by ethyl acetate and dispersed in methanol. Ethyl acetate was used to wash the nanocrystals two times to remove excess MHA and other byproducts. The purified MHA-capped CdTe NCs were dispersed in 16 mL of methanol for gelation.

Gelation of MHA-Capped and TOPO-Capped CdTe Nanocrystals. Gelation of an MHA capped CdTe sol was generally achieved by addition of 0.05 mL of a 0.3 vol % TNM methanolic solution to 4 mL aliquots ($[Cd^{2+}]$ = 0.012 M) of the MHA-capped CdTe sol.[16] The subsequent solution was shaken vigorously to obtain a homogeneous mixture. Typically, gelation was observed 3−4 h after mixing. Alternatively, gelation was achieved by photochemical methods, in which the MHA capped CdTe sol is illuminated by a mercury lamp for 9 h. The resultant gels are allowed to age 7−10 days under ambient conditions.

Gelation of a TOPO-capped CdTe sol was performed by addition of 0.05 mL 0.3 vol % TNM methanolic solution to 4 mL aliquots ($[Cd^{2+}]$ = 0.011 M) of the TOPO-capped CdTe sol. Gelation was observed 3−4 days after mixing with oxidant. The resultant wet gel was aged for 2−3 weeks under ambient conditions prior to drying.

Production of TOPO-Capped and MHA-Capped CdTe Aerogels. TOPO-capped and MHA-capped CdTe AGs were obtained by exchange of the aged wet gels with acetone 4−5 times per day for two days, followed by supercritical CO_2 drying with a SPI-DRY model critical point dryer. In the typical drying process, the acetone washed monolithic wet gels are loaded into the supercritical dryer boat under acetone and subsequently immersed in liquid CO_2 at 19 °C for 5−6 h. Subsequently, the temperature is raised to 39 °C, and the pressure automatically increases to 1300−1400 psi. The gel is maintained under these conditions for 30 min to stabilize formation of the supercritical fluid. Monolithic aerogels are obtained by venting the system over 30−40 min to remove supercritical CO_2 from the gel while maintaining the temperature.

Dispersion Studies. Thiolate solutions of MHA were prepared for dispersion studies by dissolving 0.1443 g of MHA in 5 mL of methanol followed by addition of TMAH to drive the pH to >10. TOPO-capped CdTe aerogel (∼10 mg) was dispersed in the above MHA solution. Ethyl acetate was used to precipitate the dispersed nanocrystals. The resultant nanocrystals were washed by ethyl acetate once more to remove excess thiolates and dispersed in 4 mL of methanol to obtain a nanocrystal sol for TEM evaluation.

Characterization Techniques. *Powder X-ray Diffraction (PXRD).* A Rigaku RU 200B X-ray diffractometer with a Cu Kα rotating anode source was employed for powder X-ray diffraction measurements. Powder aerogel samples were deposited on a zero background quartz holder coated with a thin layer of grease. X-ray diffraction patterns were identified by reference to the phases in the International Centre for Diffraction Data (ICDD) powder diffraction file (PDF) database (release 2000).

Transmission Electron Microscopy (TEM)/Energy Dispersive Spectroscopy (EDS). The TEM analysis was performed in bright field mode by using a JEOL 2010 HR analytical electron microscope operating at a 200 kV acceleration voltage. Finely powdered aerogel samples were dispersed in acetone followed by sonication. One drop of the solution was added onto a carbon-coated copper TEM grid, and the solvent was allowed to evaporate prior to introduction to the instrument.

Semiqualitative elemental compositions of CdTe NCs and the resultant AGs were obtained using an *in situ* energy dispersive spectroscopy (EDS) unit (EDAX, Inc.) attached to the transmission electron microscope.

Surface Area and Porosimetry Analysis. Surface area and porosimetry profiles of powdered CdTe AGs were obtained from nitrogen adsorption/desorption isotherms acquired at 77 K on an ASAP 2010 surface area and porosimetry analyzer from Micromeritics. The surface areas of the aerogels were calculated by using the Brunauer–Emmett–Teller (BET) model. The Barrett–Joyner–Halenda (BJH) model was used to generate a pore-size distribution plot and calculate the average pore diameter and cumulative pore volume. Aerogel samples were degassed under vacuum at 100 °C for 48 h before analysis.

Diffuse Reflectance UV–Vis Spectroscopy. A Jasco V-570 UV–vis–NIR spectrophotometer equipped with an integrating sphere was used to measure the optical diffuse reflectance of CdTe AGs. A small amount of powder was spread evenly on the sample holder and measured from 1000 to 200 nm (1.24–6.2 eV). The baseline was corrected by a reflectance standard ($BaSO_4$). The reflectance data were converted to absorption to yield the optical absorption spectra according to the Kubelka–Munk equation.[30]

Photoluminescence. A Cary Eclipse (Varian, Inc.) fluorescence spectrometer was used for studying emission properties of nanocrystals and aerogels. Nanocrystal solutions were loaded in a 1 cm quartz fluorescence cell, and analyses were conducted under ambient conditions. Powder aerogel samples were sealed in evacuated quartz tubes, and analyses were conducted at liquid nitrogen temperature.

Atomic Absorption Spectroscopy. A Perkin-Elmer AAnalyst 700 atomic absorption spectrometer equipped with flame and graphite furnace atomizers was employed for determination of Cd concentration, $[Cd^{2+}]$, in solutions of nanocrystals and in aerogel samples. The air–acetylene flame technique was used. Samples were prepared by dissolution in 2 vol % HNO_3 solution. $[Cd^{2+}]$ of five standard solutions was measured to establish a calibration curve, and a 2 vol % HNO_3 blank solution was used to correct the background signal.

RESULTS

Synthesis and Assembly of CdTe Nanocrystals. Trioctylphosphine oxide (TOPO) -capped CdTe NCs were prepared by arrested precipitation using a literature method.[28] The phase was confirmed to be that of hexagonal CdTe by PXRD (Figure 1), with a crystallite size of 4.4 nm (calculated from the application of the Scherrer equation to the peak at 39° 2θ). A portion of the nanocrystals was subjected to surface exchange with thiolate ligands under basic conditions (pH > 10). Intriguingly, our standard thiol employed in exchange, 11-mercaptoundecanoic acid (MUA), resulted in transformation of the red CdTe sol into a black precipitate, identified as crystalline Te by PXRD (Figure S1). Accordingly, a longer chain thiol, 16-mercaptohexadecanoic acid (MHA) was explored and found to yield stable thiolate-capped sols. Gelation of the MHA-capped CdTe NCs was achieved via oxidative removal of the surface thiolate groups by use of a chemical oxidizing agent (tetranitromethane, TNM). Use of 0.025 mL of 3 vol % of TNM methanol solution (resulting in the concentration ratio of TNM to Cd^{2+} equal to 1:8)[31] led to gelation, but this was accompanied by bleaching, resulting in a white gel. In contrast, 0.05 mL of 0.3 vol % TNM ($[TNM]:[Cd^{2+}] = 1:40$) led to slow gelation over 3–4 h with no loss of the deep red color. The resultant wet gel was aged for 7 days under ambient conditions to obtain a robust monolithic wet gel. For comparison, photooxidation of a MHA-capped CdTe nanocrystal sol by mercury lamp illumination was explored for gelation.

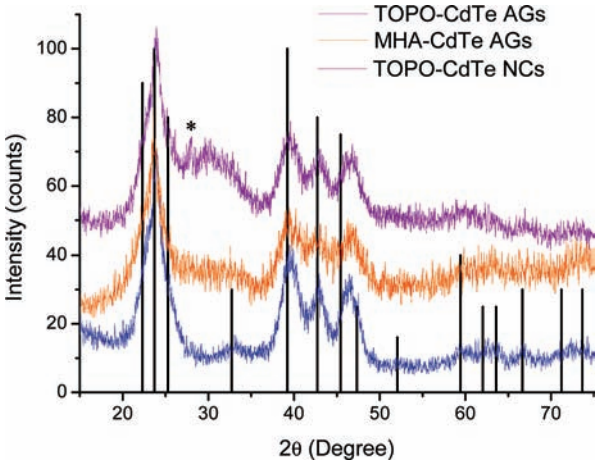

Figure 1. PXRD pattern of TOPO-capped and MHA-capped AGs and of TOPO capped CdTe NCs. The ICDD-PDF overlay of hexagonal CdTe (PDF 19-0193) is shown as vertical lines. * indicates the most intense reflection of crystalline Te.

TOPO-capped CdTe NCs can be directly assembled into gels without first undergoing surface exchange with thiolate. This was achieved by redispersing the as-prepared nanocrystals with toluene and reprecipitating them with methanol two times prior to addition of TNM. As for the MHA-capped CdTe gelation, 0.05 mL of 0.3 vol % TNM was applied to 4 mL of TOPO-capped nanocrystal sol to achieve a concentration ratio of $[TNM]:[Cd^{2+}]$ equal to 1:40. The first sign of gelation (viscosity change) was observed in 3–4 days, and complete gelation (clear supernatant) required 3 weeks.

Structure and Porosity of CdTe Aerogels: TOPO- vs MHA-Capped Precursors. Wet gels were exchanged with acetone to remove reaction byproducts and dried via supercritical CO_2 extraction to produce aerogels. As shown in Figure 1, the PXRD patterns of the AGs resulting from TOPO-capped or MHA-capped CdTe NCs are identical and consistent with the hexagonal CdTe crystal structure of their primary TOPO-capped CdTe NCs. Moreover, the peak breadths are essentially identical for all materials studied, suggesting the crystallite size has not changed. The small peak at 27.9° in the PXRD of the TOPO-capped aerogel is attributed to a small amount of crystalline Te, while the broad peak at 30° might be due to an amorphous component produced during the depassivation process in the synthesis of the TOPO-capped aerogel.

Transmission electron microscopy was employed to study the morphology of the CdTe AGs assembled from TOPO-capped and MHA-capped NCs (Figure 2). The two aerogels exhibit similar colloidal morphologies with a broad range of pores extending from the microporous (<2 nm), through mesoporous (2–50 nm), and into the macroporous (>50 nm) regime. HRTEM images of the two aerogels demonstrate the presence of interconnected networks composed of nearly spherical NCs. Lattice fringes clearly show the nanoscale building blocks to be highly crystalline. These can be indexed to hexagonal CdTe in both aerogels.

Elemental compositions (Cd, Te, P, and S) of the precursor nanocrystals and TOPO-capped and MHA-capped CdTe AGs are shown in Table 1. The Cd to Te ratio is approximately 1:1 in the primary nanocrystals and the assembled forms, consistent with the formulation of CdTe. The P content of the twice toluene

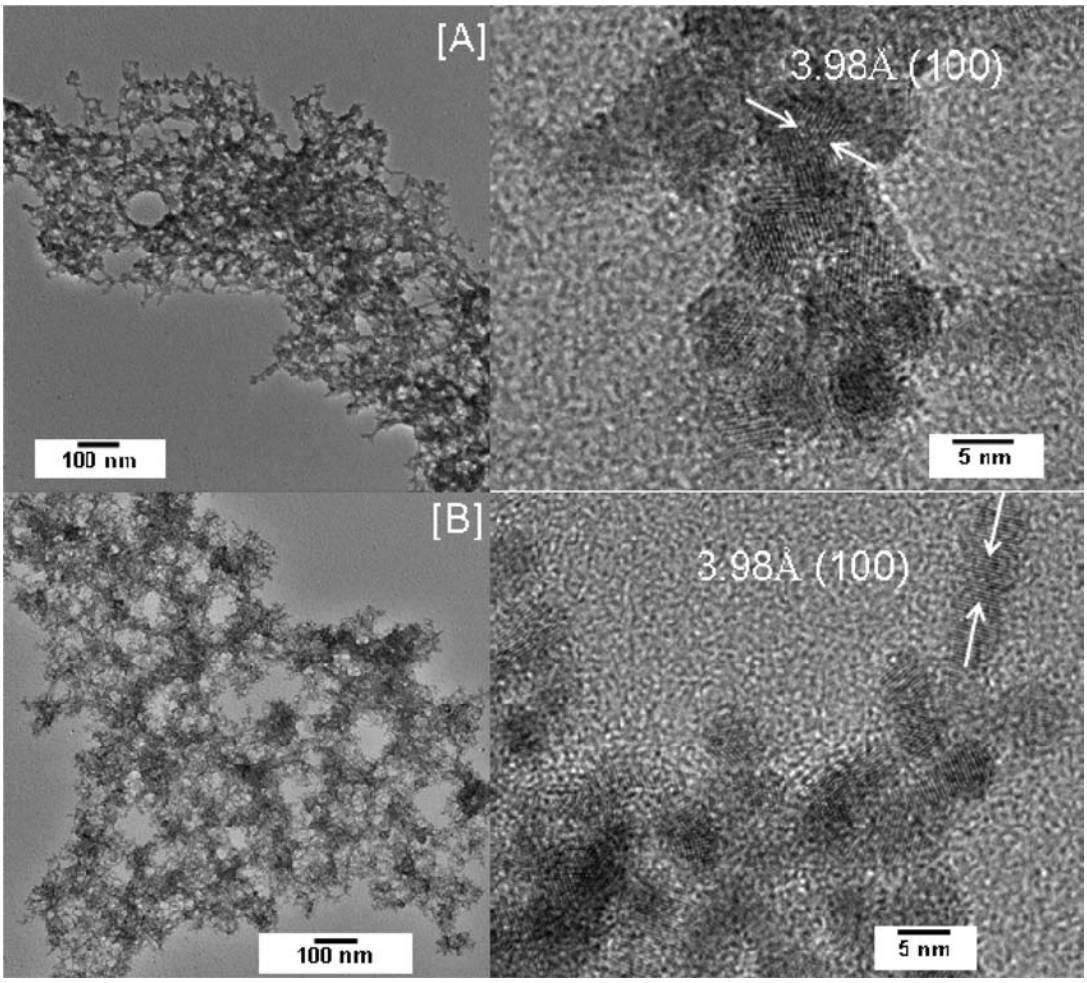

Figure 2. TEM images of MHA-capped (A) and TOPO-capped (B) aerogels (left, low resolution; right, high resolution). Groups of lattice fringes, and their corresponding *d*-spacing and indices, are shown in the high resolution images.

Table 1. Energy Dispersive Spectroscopy Data on CdTe Nanocrystals and Aerogels

	elemental composition (at. %)				
sample	Cd	Te	P	S	atomic ratio
TOPO-CdTe NCs	42.8	40.2	17.0	ND	Cd:Te:P 1:0.93:0.40
dispersed/reprecipitated TOPO-CdTe NCs	46.5	46.2	7.3	ND	Cd:Te:P 1:0.99:0.16
TOPO-CdTe AGs	48.2	45.9	5.9	ND	Cd:Te:P 1:0.95:0.12
MHA-CdTe NCs	39.3	35.8	6.5	18.4	Cd:Te:P:S 1:0.91:0.16:0.46
MHA-CdTe AGs	47.2	45.8	1.0	6.0	Cd:Te:P:S 1:0.97:0.02:0.13

dispersed/reprecipitated TOPO-capped NCs was decreased to 7.3 at. % from 12.2 at. % in the as-prepared nanocrystals due to the partial removal of TOPO ligands during the dispersion/reprecipitation process. This value is further reduced to 5.9% in the aerogel, presumably due to loss of even more TOPO from the particle surface during the oxidation process. In the case of thiolate-capped systems, a substantially decreased P content confirmed that the majority of the TOPO ligands were replaced by MHA capping groups. A small of amount of S was still observed in the MHA-capped CdTe aerogel, attributed to the presence of residual thiolate functionalities on the surface of the aerogels.

Porosimetry characteristics of the aerogels were determined by N_2 adsorption/desorption isotherms. Isotherms of the AGs formed from MHA-capped and TOPO-capped CdTe NCs demonstrate a type IV curve, which is characteristic of a mesoporous material, and are similar in shape (Figure S2). The calculated BET surface areas of the TOPO-capped and MHA-capped CdTe aerogel are comparable to a "traditional" silica aerogel (600 m^2/g) when converted to silica equivalence by normalization for density differences (Table 2). A broad pore size distribution is indicative of meso- to macroporosity in both of the aerogel materials (Figure S3), consistent with a highly porous structure as revealed by electron micrograph images (Figure 2).

dx.doi.org/10.1021/ic201333y |*Inorg. Chem.* 2011, 50, 9985–9992

Table 2. Porosimetry Data for CdTe Aerogels[a]

sample	BET surface area (m^2/g)	silica equivalence BET surface area (m^2/g)[b]	BJH average pore diameter (nm)	BJH cumulative pore volume (cm^3/g)
TOPO-CdTe AGs	143 ± 23	568 ± 92	12.7 ± 0.7	0.83 ± 0.12
MHA-CdTe AGs	120 ± 6	476 ± 25	13.8 ± 3.2	0.55 ± 0.04

[a] Values represent the average of two samples for TOPO-CdTe, and three for MHA-CdTe. [b] Silica equivalence surface areas were computed by converting the BET surface area for 1 mol of CdTe aerogel into that for 1 mol of SiO_2 using respective compound formula masses.

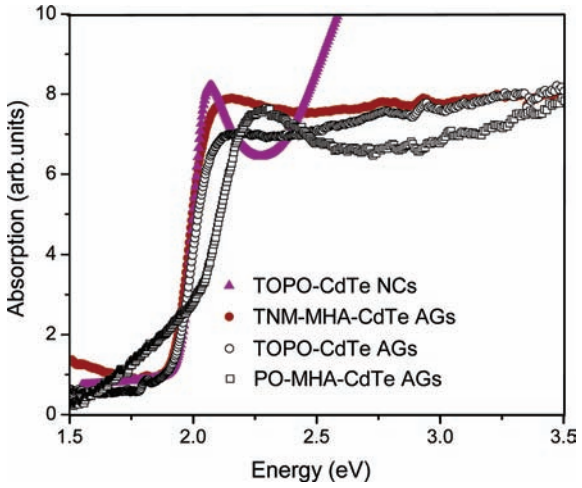

Figure 3. Optical absorption (data converted from diffuse reflectance) spectra of TOPO-capped NCs (▲), TNM oxidized MHA-capped AGs (■), TOPO-capped aerogel (○), and photo-oxidized (PO) MHA-capped AGs (□).

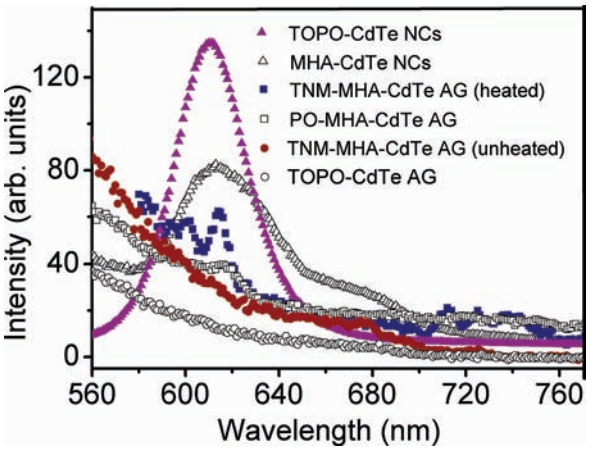

Figure 4. Photoluminescence spectra of TOPO-capped (▲) and MHA-capped (△) CdTe NCs, and heated TNM oxidized MHA-capped CdTe AGs (■), photo-oxidized (PO) MHA-capped CdTe AGs (□), unheated TNM oxidized MHA-capped CdTe AGs (●), and TOPO-capped CdTe AGs (○).

Within the error of the measurements, the porosity characteristics are reproducible from sample to sample, with standard deviations on the order of 5−20% (Table 2).

Optical Properties of CdTe Aerogels: TOPO- versus MHA-Capped Precursors. The optical energy band gap values of CdTe AGs were measured as the onsets of the optical absorption spectra converted from diffuse reflectance measurements (Figure 3). The TOPO-capped and MHA-capped aerogels exhibit identical band gaps at 1.92 eV, a value which is significantly higher than that of bulk CdTe, 1.50 eV, demonstrating that the aerogels are effectively quantum confined. These band gap energy values are slightly red-shifted compared to the energy value (1.95 eV) of the nanocrystal precursor.

In an effort to assess the effect of gelation strategy, chemical oxidation vs photo-oxidation, on photophysical properties, the band gap of a photo-oxidized (PO) MHA-capped aerogel was also evaluated (Figure 3). The obtained band gap was 2.02 eV, which is considerably larger than that for TNM oxidized MHA-capped aerogel (1.92 eV) or even for the precursor nanocrystals (1.95 eV). Moreover, there is a pronounced absorbance tail into the red.

Photoluminescence studies on the as-prepared TOPO-capped CdTe NCs reveal an emission at 610 nm (Figure 4), near the band-edge (635 nm). This is retained in the MHA-capped nanocrystal products but with a decreased relative intensity and the addition of a broad peak centered at 680 nm (Figure 4). This new peak is attributed to the presence of surface hole traps due to the thiolate capping functionalities. In contrast, the luminescence of the TNM oxidized MHA-capped CdTe AGs, as well as the TOPO-capped AGs, is fully quenched. However, two relatively sharp features at 600 and 615 nm near the band edge (645 nm) can be obtained by heating the TNM oxidized MHA-capped CdTe AGs at 100 °C under high vacuum (Figure 4). Photo-oxidation of MHA-capped CdTe NCs leads to aerogels with broad features at 595 and 615 nm, suggesting photoxidation may lead to inherently more photoluminescent aerogels.

Dispersion Studies. The reversibility of the gelation process (dispersion) was probed by chemical reduction. Dispersion studies were conducted by addition of a methanolic solution of MHA/TMAH (pH > 10) to the TOPO-capped CdTe AGs. The recovered nanocrystal sols were visually identical to the primary nanocrystal sol. Evaluation of the product by TEM revealed that the gels had been converted to finely dispersed NCs (Figure S3).

■ DISCUSSION

Comparison of CdTe Aerogels to CdS and CdSe Aerogels. Typically, formation of CdS or CdSe AGs involves (1) preparation of trioctylphosphine oxide capped NCs; (2) surface exchange with thiolate capping ligands; (3) oxidative loss of thiolate ligands; and (4) oxidative gelation of nanocrystals. The thiol of choice is MUA because the relatively long chain acts as a good stabilizer, making the surface less accessible to oxygen and hence resistant to spontaneous photoinduced aggregation. The relatively stable sol can then be transformed to a gel when ready by addition of chemical oxidants.

A key difference in the preparation of CdTe AGs relative to CdSe and CdS AGs is the amount and concentration of oxidants used for gelation of the MHA capped CdTe NCs relative to that

dx.doi.org/10.1021/ic201333y |Inorg. Chem. 2011, 50, 9985–9992

for MUA capped CdS and CdSe NCs. When the same concentration ratio of TNM to Cd^{2+} (1:8), used for gelation of CdS and CdSe NCs, was initially applied to the CdTe nanocrystal solution, a compact and white gel was formed. The shrinkage of the gel network indicates the oxidizer to thiolate ratio (x = [TNM]/[MHA]), which controls the number of reactive surface sites, as proposed by Gacoin et al.,[32] is too big. The presence of excess oxidant causes formation of new interparticle bonds after gelation, due to the presence of excess reactive sites, thus leading ultimately to shrinkage of the gel network. In contrast, a decreased ratio ([TNM]/[Cd^{2+}] = 1/40) was found to efficiently lead to slow and controlled gelation after 3−4 h. The fact that the same relative concentration of TNM successfully used for CdS and CdSe with minimal syneresis (V_{gel}/V_{sol} = ca. 60−80%) causes significant CdTe gel shrinkage (V_{gel}/V_{sol} = ca.10−20%) may be explained by the lower redox potential for Te^{2-} relative to Se^{2-} and S^{2-}, leading to a greater number of bonds formed between particles. The bleaching phenomenon (observation of a white gel from a red sol) was not mentioned in Gacoin et al.'s study[32] of CdS, even when the oxidant concentration was high (x > 0.8). However, Eychmüller and co-workers[25] did observe similar bleaching of CdTe gels at high oxidant concentration. The color change is likely due to formation of tellurates (TeO_4^{2-}), which are reported to form upon reaction of telluride or tellurium with oxidizing agents (e.g., H_2O_2, or chromic acid).[33] Again, this observation is consistent with more facile oxidation of Te^{2-} relative to S^{2-} or Se^{2-}.

Another difference in the synthesis of CdTe AGs relative to CdS and CdSe AGs is that MHA is used as the thiolate stabilizer for surface exchange of TOPO-capped CdTe NCs instead of MUA, as is used for CdS and CdSe NCs. The latter was found to yield elemental Te (as revealed by PXRD) when combined with the TOPO-capped CdTe sol. While the origin of this phenomenon is not clear, it is possible that an adventitious oxidant is introduced with MUA. This is also consistent with a greater susceptibility to oxidation on the part of CdTe relative to CdS and CdSe where no such problems were encountered during MUA capping.

Effect of Capping Ligand on Gelation: Mechanism and Properties of the Resultant Aerogels. If interparticle perchalcogenide bond formation is responsible for gelation of CdTe, as previously demonstrated for CdSe and CdS, the critical step in gel formation is exposure of Te^{2-} to the oxidant. Thus, thiolate-capping should not be a prerequisite to gel formation, providing surface ligands and metal ions can be sufficiently removed to expose chalcogenide. Accordingly, we probed the suitability of TOPO-capped NCs as gel precursors. A critical step is removal of a portion of the surface groups to expose Te^{2-} for oxidation. This is achieved by two cycles of dispersion with toluene followed by reprecipitation of the nanocrystals with methanol to obtain a moderately depassivated nanocrystal surface, followed by the chemical oxidation reaction. It was found that a single dispersion/reprecipitation step yielded a sol that was resistant to gelation, while dispersion/reprecipitation more than twice, or with strong TOPO solubilizing solvents (i.e., chloroform), produced precipitates (i.e., the precursor particles could not be redispersed to form a sol). The gel-resistant sol suggests an insufficient depassivation on the nanocrystal surface, whereas precipitate formation indicates a near complete decomplexation of the capping ligands from particle surface.

Whereas MHA-capped CdTe nanocrystal sols start to gel in 3−4 h and form a stable monolith after a further 7−10 days of aging, the TOPO-capped NCs require 3−4 days before an apparent viscosity change is even observed, and subsequent aging is generally performed over 3 weeks to obtain complete gelation (clear supernatant). The slower process of TOPO-capped CdTe gel formation suggests the gelation process for TOPO-capped CdTe NCs is not as efficient as that for MHA-capped nanocrystals. In the latter case, the presence of an oxidant during ligand (thiolate) removal enables the exposed CdTe surface to immediately react, whereas ligand removal occurs as a separate step in the gelation of TOPO-capped nanocrystal sol, perhaps enabling some kind of surface chemical rearrangement or reaction that makes the particles less susceptible to oxidative gelation. However, when comparing all the collected data on the characterization of as-prepared TOPO-capped and MHA-capped AGs, the physicochemical properties of both of the materials are found to be nearly identical in terms of structure, morphology, crystallinity, quantum confinement effect, surface area, and porosimetry. The similarity of properties of TOPO-capped and MHA-capped CdTe AGs indicates that ligation on the nanocrystal surface does not have a major effect on the gelation process as long as proper depassivation of the particle surface is achieved, consistent with the finding in the mechanism study[21] for gelation of CdSe NCs, where surface thiolate groups are oxidatively removed first but oxidation of the subsequently exposed surface chalcogenides is the step responsible for network formation. Moreover, these data suggest that the gelation itself can not involve any cross-linking thiolate linkages, as was observed in the TGA-Cd or tetrazolyl-Cd gels prepared by Eychmüller and co-workers.[26,27]

On the basis of the data presented above, we propose a similar mechanism to that responsible for gelation of CdSe is occurring in the MHA-capped and TOPO-capped NCs, as shown in Scheme 1. Activation is achieved either by oxidative removal of surface thiolate capping groups after exchange of TOPO-capped CdTe NCs with thiolates (Scheme 1, PATH-1) or by dispersion of TOPO-capped CdTe NCs with toluene/reprecipitation with methanol two times to remove surface TOPO ligands and/or Cd-TOPO species (Scheme 1, PATH-2). Both of the actions are expected to lead to a Te-rich surface. Upon oxidation, Te^{2-} is then oxidized to $Te^{\bullet -}$ species that can combine with species on other particles to form $(Te_2)^{2-}$ or $(Te_n)^{2-}$ linkers between particles, leading to gelation. As shown with the dispersion studies, these $(Te_n)^{2-}$ linkages can be reduced by thiolate, reforming the sol, confirming the oxidized state of interfaces within the gel network.

Comparison of Current Results to Previous Studies on CdTe Gels. The study by Gaponik, Eychmüller, and co-workers' produced gels by chemical oxidation methods that are similar to our findings. Specifically, they observed PL quenching for the gels produced by H_2O_2 oxidation of NCs and bleaching phenomenon when the H_2O_2 concentration is high. However, their UV-light illuminated (photo-oxidized) gels and aerogels were found to be highly photoluminescent. Therefore, we performed a study on the effect of chemical versus photo-oxidative gelation on the photophysical properties of aerogels. However, the aerogel prepared from supercritical drying of our photo-oxidized gel actually has a wider gap than the precursor nanocrystals, suggesting surface etching or oxidation (i.e., smaller chromophore size). While peaks due to near-band-edge PL are discernible, the PL is weak and not evident to the naked eye, as is the case for the gels produced by Gaponik et al. The poor PL properties of the prepared CdTe AGs in this study might be due to overoxidation of the CdTe NCs either by overexposure of the CdTe NCs to

Scheme 1. Proposed Mechanism of TOPO-Capped and MHA-Capped CdTe Nanocrystal Oxidative Gelation and Reductive Dispersion

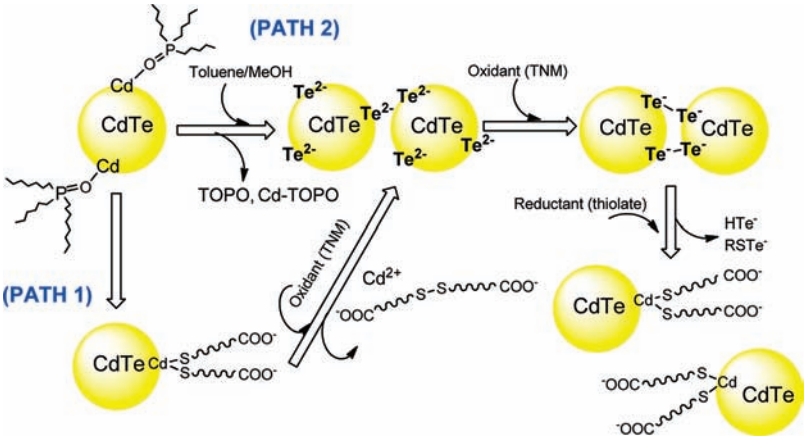

TNM or $h\nu/O_2$ during the gelation and aging process or the oxidants' strength being too high (in the case of TNM). Indeed, Gaponik et al. found that if slow centrifugation was employed after the first sign of gelation in either H_2O_2 oxidation or photo-oxidation gelation processes, a higher degree of PL was observed. In the former case, centrifugation was used to enhance coagulation and remove unreacted H_2O_2, hence avoiding overoxidation of nanocrystals. In the latter case, centrifugation followed by immediate washing was used to facilitate interparticle networking to shorten the photo-oxidation time (again effectively limiting oxidizing equivalents). These approaches, while rendering useful optical properties, are likely to result in sedimentation/compaction of the gel, reducing surface areas. As Gaponik et al. have not performed surface area analyses on their materials, no direct comparison can be made.

CONCLUSIONS

The present study has shown that CdTe NCs can be assembled into highly porous gels and aerogels, regardless of the surface ligation (i.e., thiolate capping is not obligatory). This suggests that the mechanism of oxidation-induced interparticle per-chalcogenide linkages postulated for CdS and CdSe is also operative for CdTe, a conclusion strengthened by the observation of reduction-induced dispersion of the gels into sols. The aerogels exhibited similar structural, morphological, and porosimetry properties, suggesting that surface ligation has no major effect on the gelation process and the resultant aerogel properties. While the aerogels remain quantum confined, the PL is highly quenched. The origin of the quenching is not clear, but is most likely related to oxidation. Future work will focus on maintaining the high surface area achieved by oxidation induced gelation while minimizing surface oxidation to preserve the photoluminescence characteristics.

ASSOCIATED CONTENT

Supporting Information. X-ray powder diffraction, N_2 adsorption/desorption isotherm plots, and electron micrographs of dispersed gels. This material is available free of charge via the Internet at http://pubs.acs.org.

AUTHOR INFORMATION

Corresponding Author
*E-mail: sbrock@chem.wayne.edu.

ACKNOWLEDGMENT

This work was supported in part by the National Science Foundation (DMR-0701161), the donors of the American Chemical Society Petroleum Research Fund (43550-AC10), and Wayne State University (WSU) Institute of Manufacturing Research. Electron microscopy data were collected on a JEOL 2010 in the WSU Central Instrumentation Facility funded in part by NSF (DMR-0216084). We thank Dr. Yi Liu for the help in acquiring TEM images.

REFERENCES

(1) Yu, W. W.; Qu, L.; Guo, W.; Peng, X. *Chem. Mater.* **2003**, *15*, 2854–2860.
(2) Murray, C. B.; Norris, D. J.; Bawendi, M. G. *J. Am. Chem. Soc.* **1993**, *115*, 8706–8715.
(3) Yu, W. W.; Wang, Y. A.; Peng, X. *Chem. Mater.* **2003**, *15*, 4300–4308.
(4) Manna, L.; Milliron, D. J.; Meisel, A.; Scher, E. C.; Alivisatos, A. P. *Nat. Mater.* **2003**, *2*, 382–385.
(5) Ma, J.; Chen, J.-Y.; Zhang, Y.; Wang, P.-N.; Guo, J.; Yang, W.-L.; Wang, C.-C. *J. Phys. Chem. B* **2007**, *111*, 12012–12016.
(6) Smith, A. M.; Nie, S. *Angew. Chem., Int. Ed.* **2008**, *47*, 9916–9921.
(7) Gaponik, N. P.; Talapin, D. V.; Rogach, A. L. *Phys. Chem. Chem. Phys.* **1999**, *1*, 1787–1789.
(8) Lin, Y.-W.; Tseng, W.-L.; Chang, H.-T. *Adv. Mater.* **2006**, *18*, 1381–1386.
(9) Bertoni, C.; Gallardo, D.; Dunn, S.; Gaponik, N.; Eychmüller, A. *Appl. Phys. Lett.* **2007**, *90*, 034107–1–3.
(10) Boyle, D. S.; Hearne, S.; Johnson, D. R.; O'Brien, P. *J. Mater. Chem.* **1999**, *9*, 2879–2883.
(11) Kosyachenko, L. A.; Mathew, X.; Motushchuk, V. V.; Sklyarchuk, V. M. *Sol. Energy* **2006**, *80*, 148–155.
(12) Deng, Z.; Zhang, Y.; Yue, J.; Tang, F.; Wei, Q. *J. Phys. Chem. B* **2007**, *111*, 12024–12031.
(13) Zhang, L.; Zou, X.; Ying, E.; Dong, S. *J. Phys. Chem. C* **2008**, *112*, 4451–4454.
(14) Bag, S.; Arachchige, I. U.; Kanatzidis, M. G. *J. Mater. Chem.* **2008**, *18*, 3628–3632.

(15) Mohanan, J. L.; Arachchige, I. U.; Brock, S. L. *Science* **2005**, *307*, 397–400.
(16) Arachchige, I. U.; Brock, S. L. *J. Am. Chem. Soc.* **2006**, *128*, 7964–7971.
(17) Arachchige, I. U.; Brock, S. L. *J. Am. Chem. Soc.* **2007**, *129*, 1840–1841.
(18) Gill, S. K.; Brown, P.; Hope-Weeks, L. J. *J. Sol-Gel Sci. Technol.* **2011**, *57*, 68–75.
(19) Gill, S. K.; Hope-Weeks, L. J. *Chem. Commun.* **2009**, 4384−–4386.
(20) Arachchige, I. U.; Brock, S. L. *Acc. Chem. Res.* **2007**, *40*, 801–809.
(21) Pala, I. R.; Arachchige, I. U.; Georgiev, D. G.; Brock, S. L. *Angew. Chem., Int. Ed.* **2010**, *49*, 3661–3665.
(22) Tang, Z.; Kotov, N. A.; Giersig, M. *Science* **2002**, *2002*, 237–240.
(23) Tang, Z.; Zhang, Z.; Wang, Y.; Glotzer, S. C.; Kotov, N. A. *Science* **2006**, *314*, 274–278.
(24) Srivastava, S.; Santos, A.; Critchley, K.; Kim, D.-S.; Podisiadlo, P.; Sun, K.; Lee, J.; Xu, C.; Lilly, G. D.; Glotzer, S. C.; Kotov, N. A. *Science* **2010**, *327*, 1355–1359.
(25) Gaponik, N.; A., W.; Marx, R.; Lesnyak, V.; Schilling, K.; Eychmüller, A. *Adv. Mater.* **2008**, *20*, 4257–4262.
(26) Chen, H.; Lesnyak, V.; Bigall, N. C.; Gaponik, N.; Eychmüller, A. *Chem. Mater.*, *22*, 2309-2314.
(27) Lesnyak, V.; Voitekhovich, S. V.; Gaponik, P. N.; Gaponik, N.; Eychmüller, A. *ACS Nano* **2010**, *4*, 4090–4096.
(28) Peng, Z. A.; Peng, X. *J. Am. Chem. Soc.* **2001**, *2001*, 183–184.
(29) Aldana, J.; Wang, Y. A.; Peng, X. *J. Am. Chem. Soc.* **2001**, *123*, 8844–8850.
(30) Frei, R. W.; MacNeil, J. D. *Diffuse Reflectance Spectroscopy in Environmental Problem-Solving*; Chemical Ruber Company: OH, 1973.
(31) Yao, Q.; Arachchige, I. U.; Brock, S. L. *J. Am. Chem. Soc.* **2009**, *131*, 2800–2801.
(32) Gacoin, T.; Malier, L.; Boilot, J.-P. *Chem. Mater.* **1997**, *9*, 1502–1504.
(33) Bouroushian, M. *Electrochemistry of Metal Chalcogenides*; Springer-Verlag: Berlin, 2010.